

Analysis of wavelength shifts reported for X-shooter spectra

S. Moehler (SDP)

June 15, 2015

Executive Summary

I investigated the causes for wavelength offsets seen in telluric lines and sky lines of extracted one-dimensional VIS and NIR X-shooter spectra (see Sect. 1) and found the following:

1. The offsets seen in telluric lines are at least partially caused by imperfect positioning of the target in the slit due to drifts in the reference pixels (Sect. 2 and 4). This affects also UVB data, where the effect is not noticeable due to lack of telluric lines.
2. The shift determined from the Automatic Flexure Compensation frames was not applied for NIR data. This has been fixed with pipeline version `xshoo-2.5.5` (Sect. 3).
3. The offsets derived from sky lines in VIS and NIR spectra change with wavelength. The effect has a peak-to-peak amplitude of about 0.3 pixel in both arms (Sect. 3, Figs. 8, p. 7 and Figs. 9, p. 8).

This should be compared to the systematic uncertainty currently recorded for the pipeline products, which is 0.02 nm (1 pixel) for VIS and 0.004 nm (0.07 pixel) for NIR data.

4. The sky line offsets in the NIR data split into two groups, depending on the slit used for the observations. The fact that the effect is seen also in arc line positions in raw arc lamp slit frames points towards a mis-positioning of the slits rather than a pipeline problem. The groups consist of the slits `0.4x11`, `0.6x11`, `0.9x11JH` on one side and `0.9x11`, `1.2x11`, `0.6x11JH` on the other side (Sect. 3 [especially 3.1] and 4). The split was introduced with the new slit wheel in July 2011. C. Martayan noticed that the two groups of slits are on two different sides of the slit wheel.

1 Introduction

There have been several reports on wavelength offsets seen in extracted one-dimensional X-shooter spectra:

1. The Austrian in-kind team reported that during their testing of the MOLECFIT package they found an average offset of 1 pixel between the predicted positions of telluric lines and the positions in the X-shooter NIR and VIS spectra (processed with pipeline version 2.0.0)¹. This is supported for the NIR arm by independent analyses of L. Origlia.
2. P. Goldoni reported that he found an average offset of about 1 pixel from NIR sky lines in observations with the `0.9x11` slit (average exposure time 10 minutes), while the offsets for VIS (`0.9x11`) and UVB (`1.0x11`, higher uncertainty due to few sky lines) were close to 0. These data were also processed with pipeline version 2.0.0 (physical model mode).

2 Offsets observed for telluric lines

I plotted the offsets found by the Austrian in-kind team vs. time, airmass and slit width and found that there seems to be a correlation between slit width and offset (see Fig. 1, p. 2), which is supported by the histograms of the offsets per slit (Fig. 2, p. 2). Table 1 (p. 2) provides the numbers for the offsets. It shows clearly that the value of 1 pixel offset for NIR data results from the fact that the most used slit was `0.9x11` which has an average offset of -1.1 pixel.

¹JIRA ticket <https://jira.eso.org/browse/PIPE-4833>

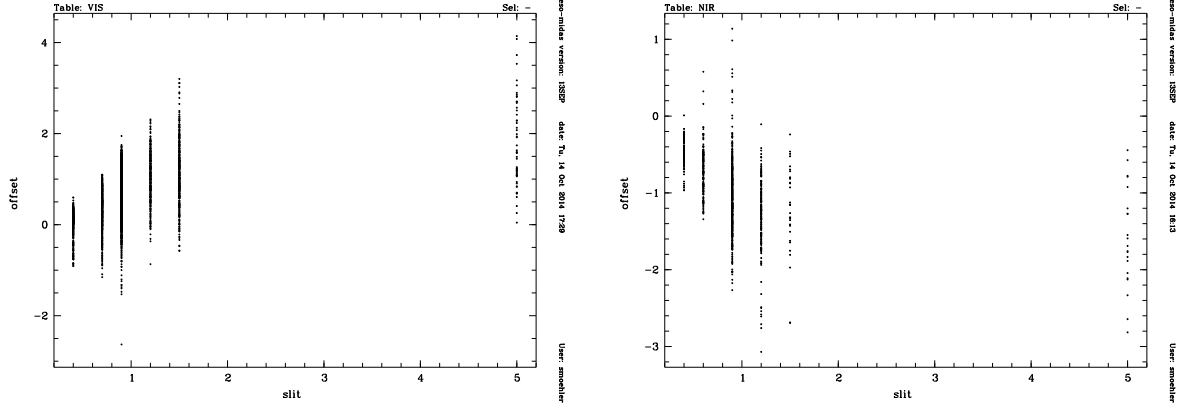


Figure 1: The plots show the offsets of the telluric lines as determined by MOLECFIT vs. slit width for the VIS (left) and NIR (right) arm.

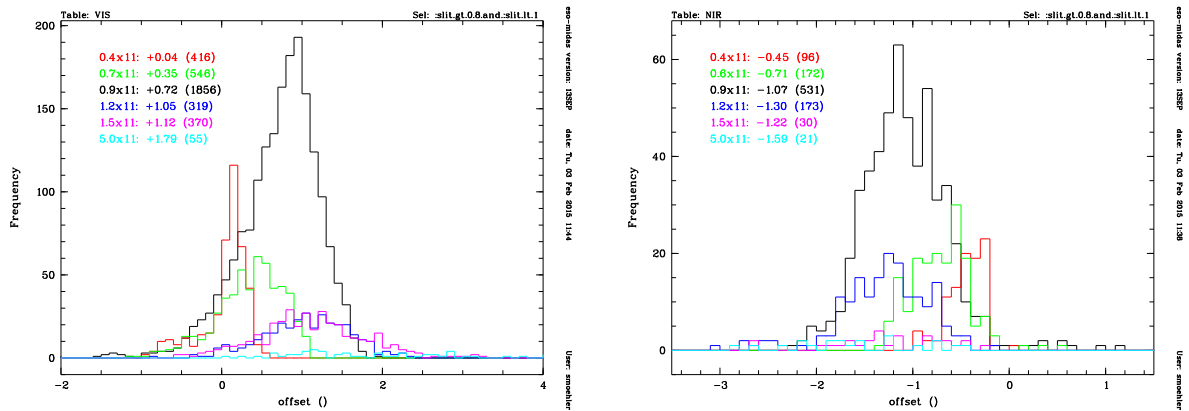


Figure 2: The plots show the histograms of offsets of the telluric lines as determined by MOLECFIT per slit for the VIS (left) and NIR (right) arm.

Table 1: Wavelength offsets in pixels of observed vs. predicted telluric lines (in pixels). The pixel size is 0.02 nm for the VIS arm and 0.06 nm for the NIR arm.

VIS				NIR			
slit	n_{obs}	mean	r.m.s	slit	n_{obs}	mean	r.m.s
0.4x11	416	+0.04	0.29	0.4x11	96	-0.45	0.19
0.7x11	546	+0.35	0.42	0.6x11	172	-0.71	0.30
0.9x11	1856	+0.72	0.49	0.9x11	531	-1.07	0.44
1.2x11	319	+1.05	0.54	1.2x11	173	-1.30	0.48
1.5x11	370	+1.12	0.67	1.5x11	30	-1.22	0.59
5.0x11	55	+1.79	0.98	5.0x11	21	-1.59	0.66

In order to verify if the offsets result from imperfect processing or flaws in the raw data I selected a pair of VIS frames that showed quite different offsets in their telluric lines (see Fig. 3, p. 3), namely XSH00.2011-10-15T00:03:53.176 (-0.871 px) and XSH00.2011-11-07T07:41:07.794 (+1.627 px). Both spectra were observed with the 0.9x11 slit. As can be seen from both Fig. 3 (p. 3) and Table 2 (p. 3), the sky lines show a much smaller difference than the telluric lines, which argues against a problem with the pipeline and favours a mis-positioning of the star in the slit as the underlying cause for the differences in the telluric line positions. The fact that the offsets correlate with the slit used suggests an incorrect relation between the star's position in the acquisition image and the slit position. As pointed out by A. Mehner (Instrument Fellow, IF) a correlation between the size of the offset and the slit width is expected even if the offset is constant, as its effect will be more noticeable for wider slits, for which the seeing will be most likely smaller than the slit width.

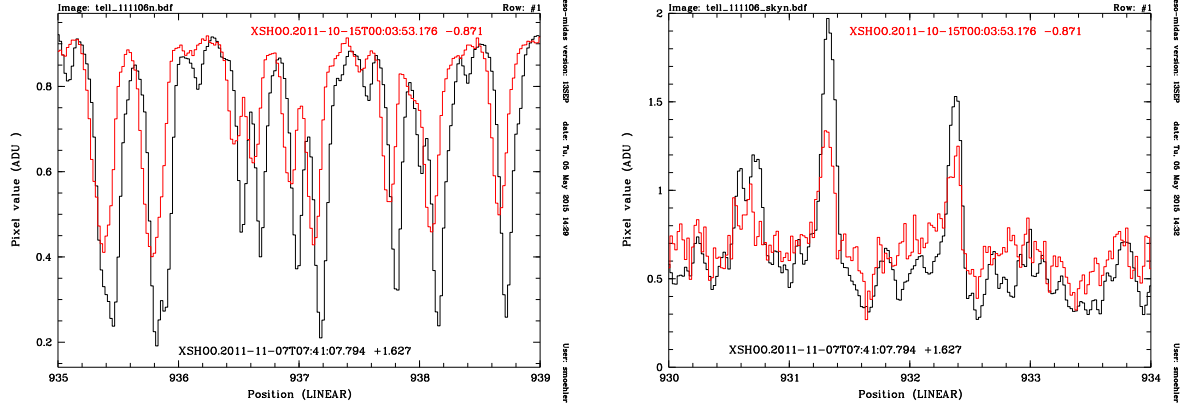


Figure 3: The plots show the telluric lines (left) and the sky lines (right) of the VIS spectra XSH00.2011-10-15T00:03:53.176 (red) and XSH00.2011-11-07T07:41:07.794 (black).

Table 2: Comparison of two VIS frames with a difference of 2.5 pixel in their telluric line positions as determined by MOLECFIT

frame	XSH00.2011-10-15T00:03:53.176	XSH00.2011-11-07T07:41:07.794
telluric_raw x [pixel]	1719.5	1717.0
telluric_raw y [pixel]	1130.5	1133.0
sky_raw x [pixel]	1725.5	1719.3
sky_raw y [pixel]	1159.8	1157.0
telluric extracted [nm]	937.747	937.805
sky extracted [nm]	931.389	931.405
(telluric-sky) extracted [nm]	6.358	6.400
telluric difference [nm]		0.058
sky difference [nm]		0.016
(telluric-sky) difference [nm]		0.042

Table 3: Results from telluric standard star observation with 0.37" offset along the dispersion axis between the two exposures. The dispersion increases along the x-axis for NIR raw data and decreases along the y-axis for raw VIS data.

VIS		
frame	XSH00.2014-10-25T00:08:13.268	XSH00.2014-10-25T00:11:12.473
telluric_raw x [pixel]	1404.941	1404.749
telluric_raw y [pixel]	1520.212	1521.060
telluric extracted [nm]	937.775	937.786
total offset raw [pixel]		0.8
total offset extracted [pixel]		0.5
total expected offset [pixel]		2.0
NIR		
frame	XSH00.2014-10-25T00:08:13.268	XSH00.2014-10-25T00:11:12.473
telluric_raw x [pixel]	449.867	449.171
telluric_raw y [pixel]	842.897	842.706
telluric extracted [nm]	1171.998	1171.969
total offset raw [pixel]		0.7
total offset extracted [pixel]		0.5
total expected offset [pixel]		1.3

To verify this scenario PSO observed a telluric standard star twice on the night 2014-10-24, applying an offset of 0.37" perpendicular to the slits between the two exposures. With pixel scales of 0.18"/pixel (VIS) and 0.28"/pixel (NIR) this should cause wavelength shifts 2.0 pixel (VIS) and 1.3 pixel (NIR). The observed data, however, show smaller offsets of about 0.7–0.8 pixels (before AFC correction, see Table 3, p. 3). This can be understood from the fact that the 0.9x11 slit was used and the seeing as stored in the

keyword `TEL.IA.FWHMLINOBS` was about $1.7''$, so that the illumination of the slits did not change very much due to the shift.

3 Offsets observed for sky lines

In order to determine potential sky line offsets in a robust and automatic manner I created NIR sky spectra with `SKYCALC`². I used a step size of 0.06 nm and a Gaussian with a FWHM of 5 pixels (for observations with the slits `0.9x11`, `1.2x11`, and `1.5x11`) and 2.5 pixels (for the slits `0.4x11` and `0.6x11`). Then I cross-correlated the region 1500 nm–2000 nm of the observed spectra with the theoretical sky spectra and fit a Gaussian to the cross-correlation peak to determine the offset. I first used spectra observed since October 2014, when X-shooter returned to UT2. For that time range I found sufficient NIR STARE slit spectroscopy data only for the slits `0.9x11` and `1.2x11`, which were then processed without sky subtraction to provide observed sky spectra. Fig. 4 (p. 4) shows the histogram of the resulting offsets. There is a clear offset and there might be a difference between the two slits.

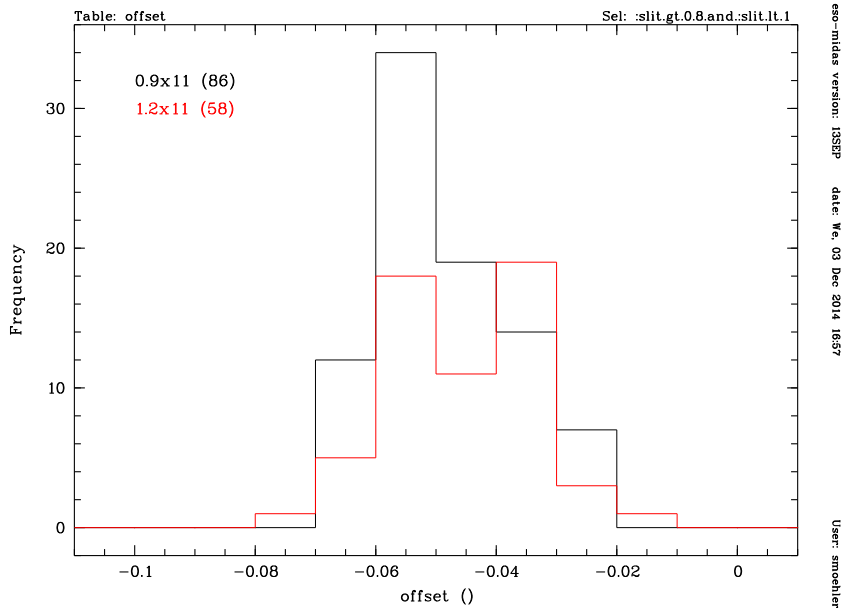


Figure 4: The plot shows the histograms of the sky line offsets in nm for NIR STARE data observed between 2014-10-01 and 2014-12-01 (1 pixel corresponds to 0.06 nm).

Next I selected some 100 NIR slit spectroscopy frames per slit from the time range 2013-10-01 to 2014-09-30, when X-shooter was at UT3, processed them as STARE data without sky subtraction and determined the offsets from their sky lines as described above. The results can be seen in Fig. 5 (p. 5). The distribution of offsets for the different slits differ, but it is not clear if this is significant.

Next I had a look at a pair of spectra, for which P. Goldoni reported a large difference in sky line positions, namely -1.65 pixels (`XSH00.2011-11-19T01:33:10.249`–`XSH00.2011-12-10T00:51:46.272`). I first compared the positions of a few selected sky lines in the raw frames and found -0.5 pixel difference along the x-axis. The processed data show a difference of -0.45 pixel, i.e. essentially the same. This was puzzling as the AFC correction for the two frames should have reduced the differential shift by at least 0.28 pixel (differential shift along x-axis). Inspecting the AFC corrected configuration tables I found them unchanged, i.e. the AFC shifts had not been applied. This was fixed by A. Modigliani (Pipeline Developer) in pipeline version `xshoo-2.5.5` on Dec. 18, 2014. Processing these specific data with the revised pipeline resulted in a differential shift measured from the sky lines of -0.08 pixels.

To verify if the lack of AFC correction is indeed responsible for the sky line shifts reported by P. Goldoni I reprocessed his data with the new pipeline version. The results are shown in Fig. 6 (p. 6). The average offset in pixel went from -0.57 px to -0.3 px and the median went from -0.77 px to -0.22 px. Plotting the shifts vs each other shows that one group with remaining large shifts (`18_off_255_px < -0.6` &&

²<http://www.eso.org/observing/etc/bin/gen/form?INS.MODE=swspectr+INS.NAME=SKYCALC>

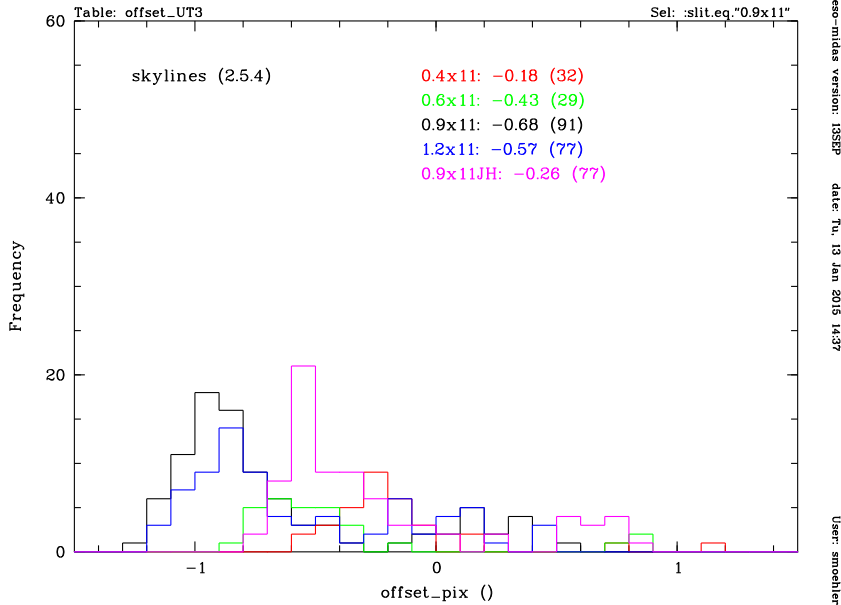


Figure 5: The plot shows the histograms of the sky line offsets (in pixels) for NIR STARE data observed between 2013-10-01 and 2014-09-30. The numbers give the average offset per slit.

$\text{off_pg_px} < 0$), while the majority of data (80) now has shifts within ± 0.5 px. If I limit the statistics to the files which have new offsets within ± 0.5 px the average moves from -0.51 px to -0.09 px and the median from -0.74 px to -0.12 px.

As a next step I processed some 450 datasets each for VIS and NIR observed between 2013-10-01 and 2014-09-30. The data sets were selected to cover as equally as possible the various slits. The data were processed without sky subtraction. Inspection of the results showed that especially for the narrow slits a significant number of objects was so bright that even without sky subtraction no sky lines could be clearly identified. These data were removed from the analysis. For the others three regions of the spectrum were correlated with the corresponding regions of the theoretical sky spectra to look for possible wavelength dependencies of any shifts: 995 nm–1045 nm, 1500 nm–1550 nm, and 1950 nm–2000 nm for the NIR arm and 650 nm–700 nm, 820 nm–870 nm, and 965 nm–1015 nm for the VIS arm. For the NIR arm I also repeated the cross-correlation used for Goldoni’s data (see Fig. 7, p. 6).

Figures 8 (p. 7) and 9 (p. 8) show the offsets for the different slits and wavelength regions, which have peak-to-peak amplitudes of about 0.3 pixels. I updated PIPE-4833 accordingly.

As A. Modigliani correctly pointed out any trend in the residuals of the `xsh_2dmap` recipe will translate into trends in the wavelength calibration of the science or standard star observations. As a test case I looked at the `xsh_2dmap` residuals for two of the demo data sets delivered with the Reflex workflow (see Fig. 10, p. 9). I noticed that the Reflex workflow has as default 2000 iterations (`model-maxit=200`), while the pipeline default is 5000 iterations (`model-maxit=500`). The argument in favour of a smaller number of iterations in Reflex was the time needed by the iterations. The recipe takes indeed about a factor of 2.5 longer with 5000 iterations (with respect to 2000 iterations), but the real time spent at that step increases from about 35 sec to 90 sec, which is acceptable within the overall time budget of a full science reduction (at least 5-6 minutes *without sky subtraction and flux calibration*). Fig. 10 (p. 9) shows that there are some differences between the residuals from 2000 and 5000 iterations, respectively. However, also with 5000 iterations trends remain. To check if a substantial increase in the number of iterations might remove the trends I repeated the processing with 200 000 and 1 000 000 iterations. For VIS data the situation indeed improves with these large numbers of iterations (see Fig. 11, p. 10, open squares), but the NIR data show hardly any change (see Fig. 12, p. 11 open squares). I also tested the effect of allowing the parameters of the physical to vary over a wider range, which, however, did not improve the results (crosses in Figs. 11, p. 10, and 12, p. 11).

To verify if the skyline shifts are reduced by using `model-maxit=500` I reprocessed the VIS data with this value. The resulting average offsets, however, changed by at most 0.02 pixel, so that the substantial shifts observed at the red end of the VIS spectra are hardly affected.

As I could not identify any clear cause for the trends observed in the wavelength calibration residuals I

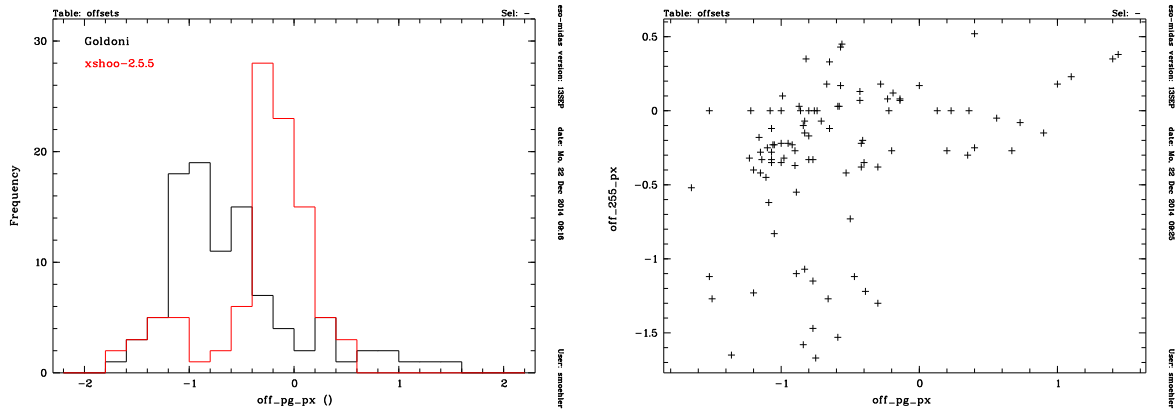


Figure 6: The left plot shows the histograms of the sky line offsets (in pixels) for NIR STARE data used by P. Goldoni for his investigations (black: Goldoni's results with pipeline version `xshoo-2.0.0`, red: my results with pipeline version `xshoo-2.5.5`). The right plot shows the offsets (in pixels) obtained with `xshoo-2.5.5` vs. those obtained with `xshoo-2.0.0`.

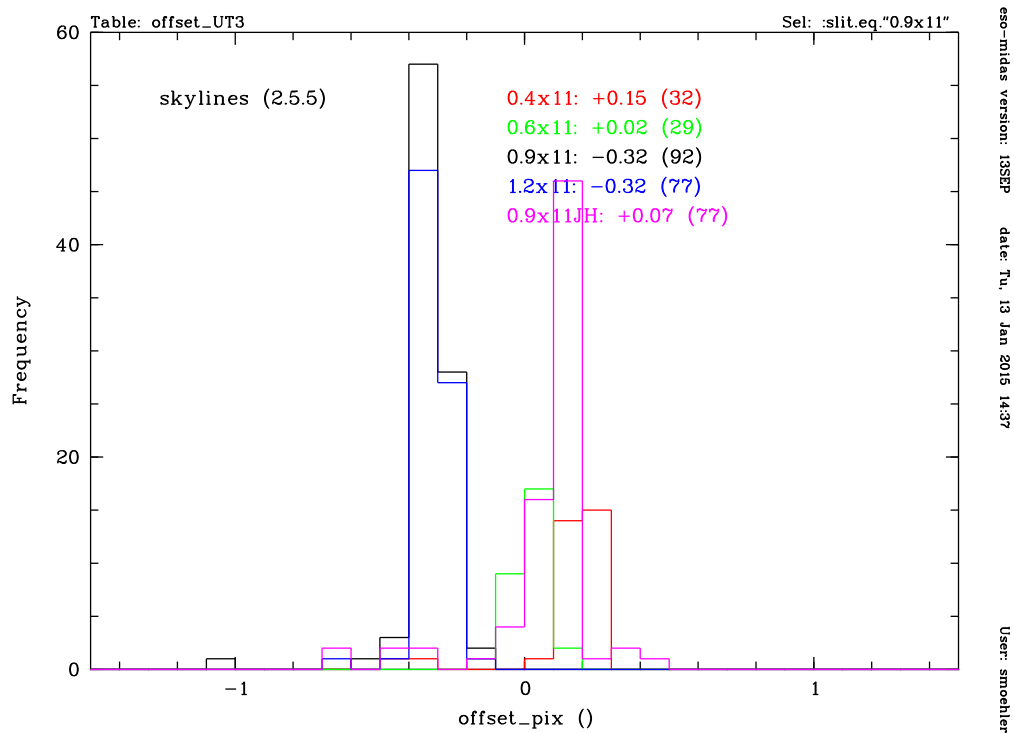


Figure 7: The plot shows the histograms of the sky line offsets (in pixels) for NIR STARE data observed while X-shooter was at UT3, which were processed with version 2.5.5.

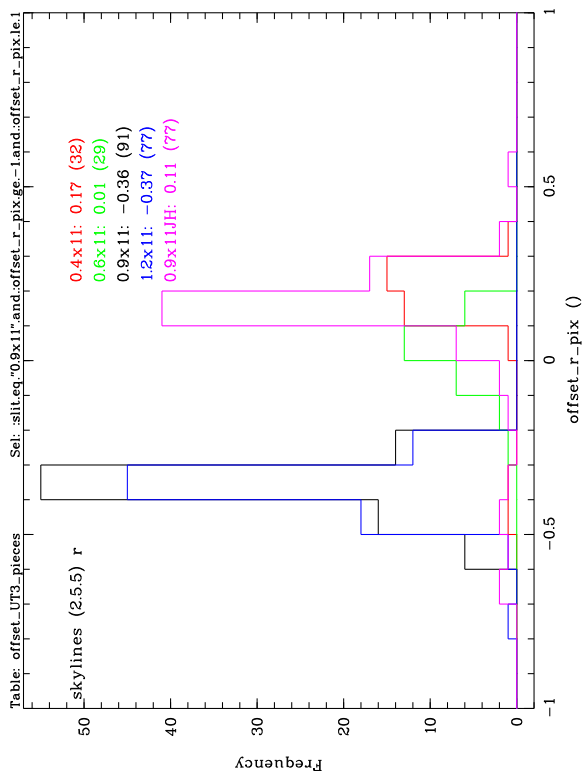
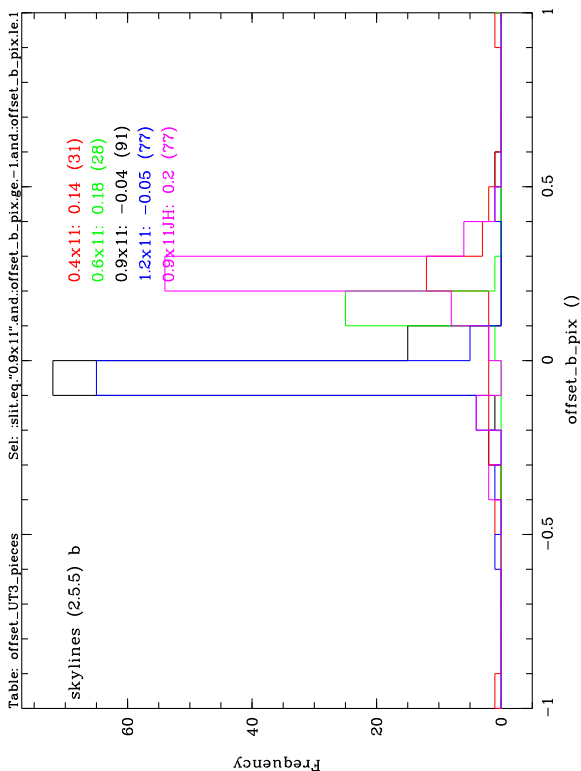
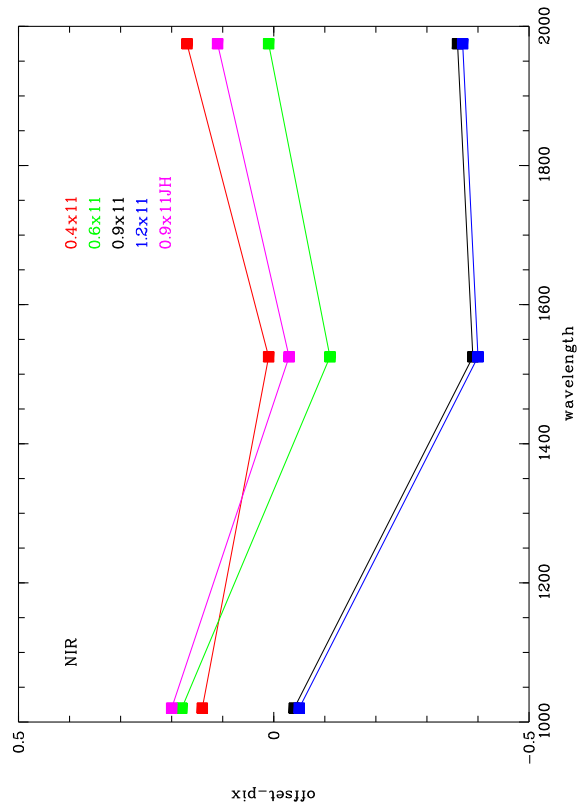
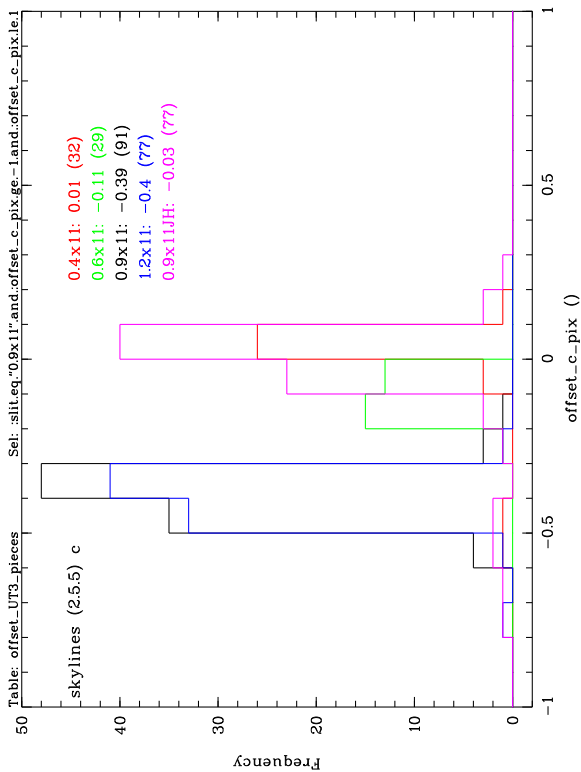


Figure 8: The plots show the histograms of the sky line offsets (in pixels) for NIR STARE data observed while X-shooter was at UT3 and processed with version 2.5.5. The offsets were determined at 1020 nm (**bottom left**), 1525 nm (**top left**), and 1975 nm (**bottom right**). The **top right** plot shows the average offsets (in pixels) vs. wavelength (in nm) for the various slits. 1 pixel corresponds to 0.06 nm.

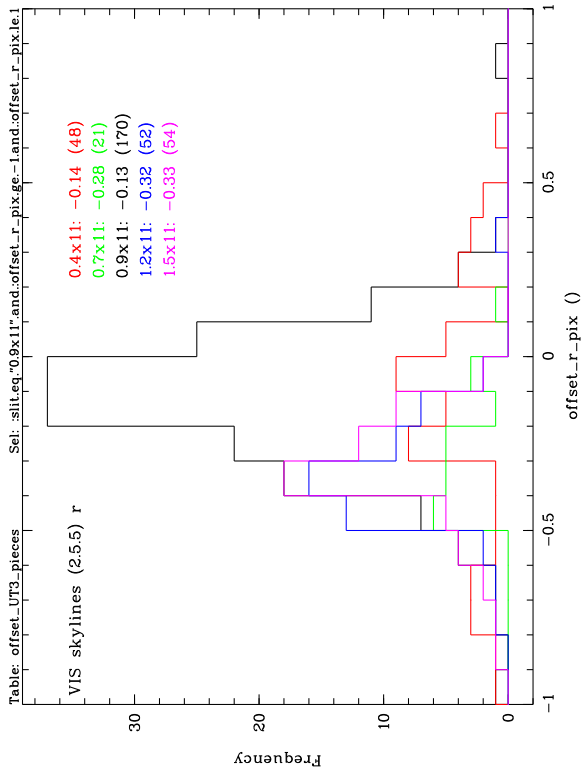
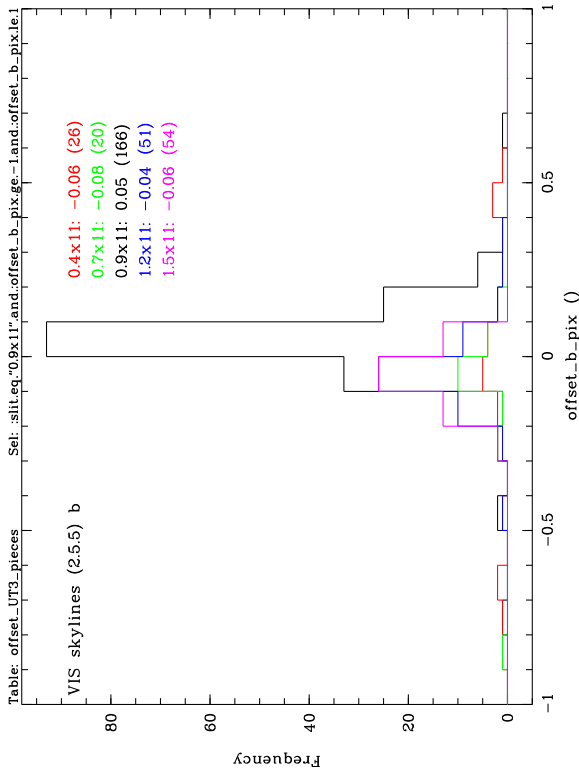
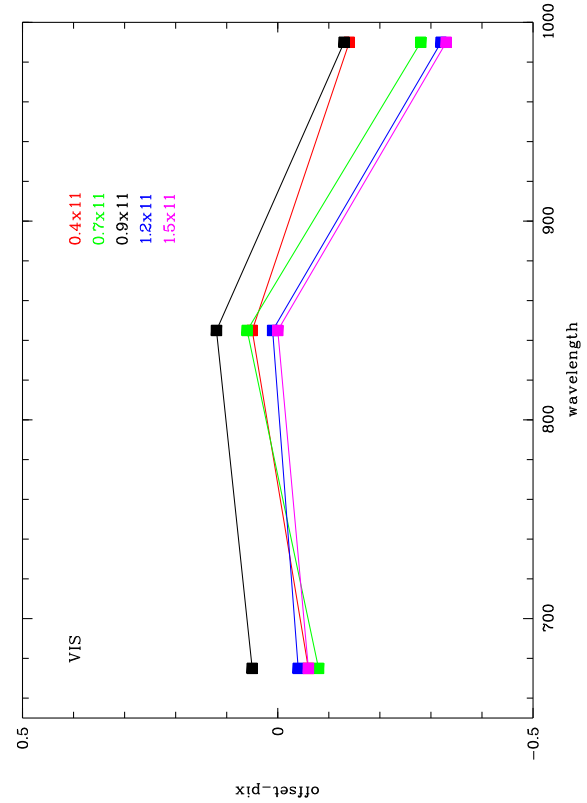
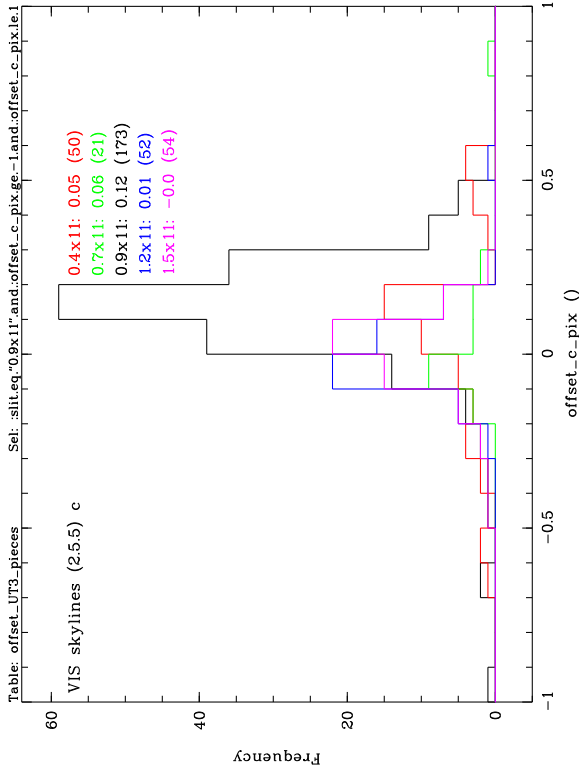


Figure 9: The plots show the histograms of the sky line offsets (in pixels) for VIS STARE data observed while X-shooter was at UT3 and processed with version 2.5.5. The offsets were determined at 675 nm (**bottom left**), 845 nm (**top left**), and 990 nm (**bottom right**). The **top right** plot shows the average offsets (in pixels) vs. wavelength (in nm) for the various slits. 1 pixel corresponds to 0.02 nm.

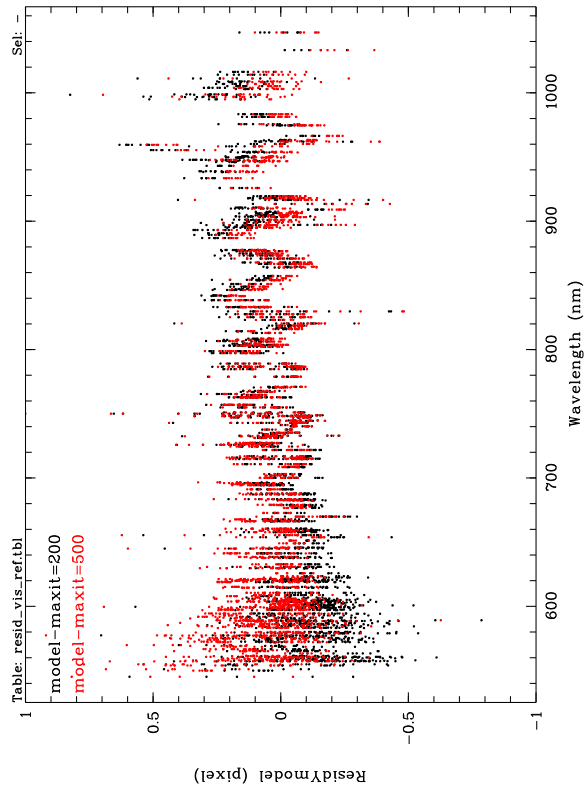
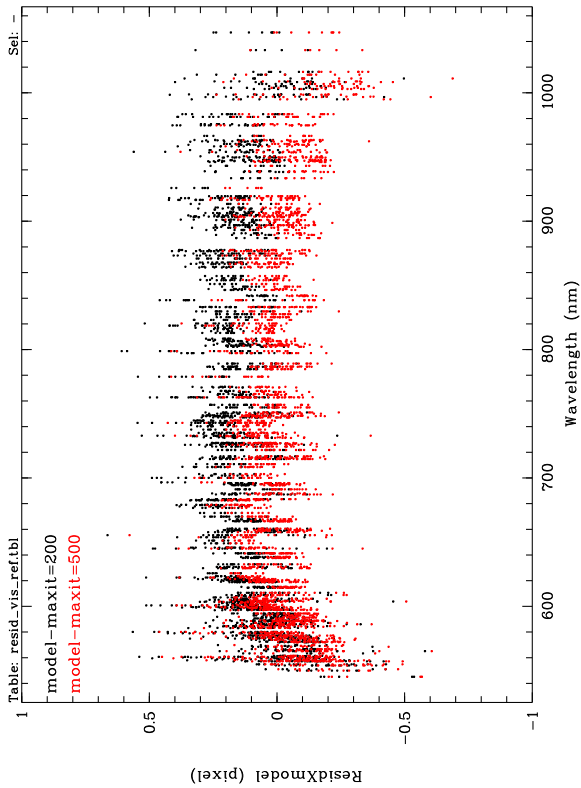
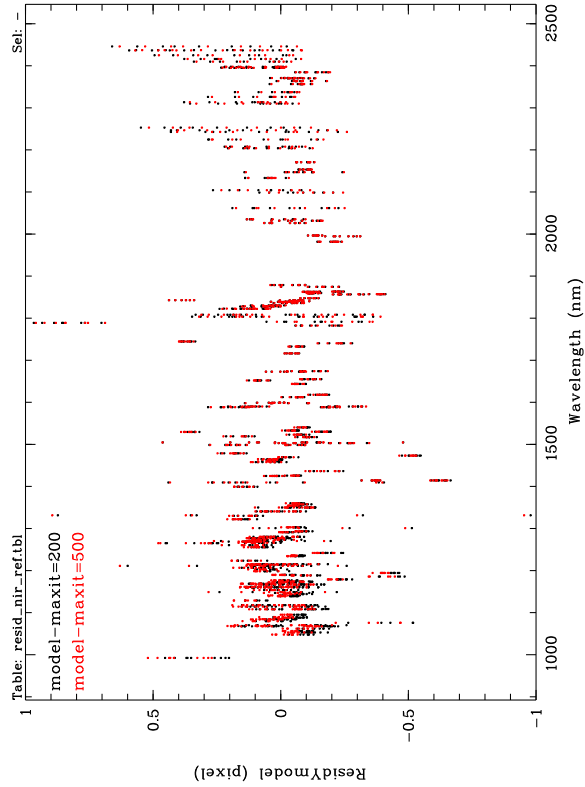
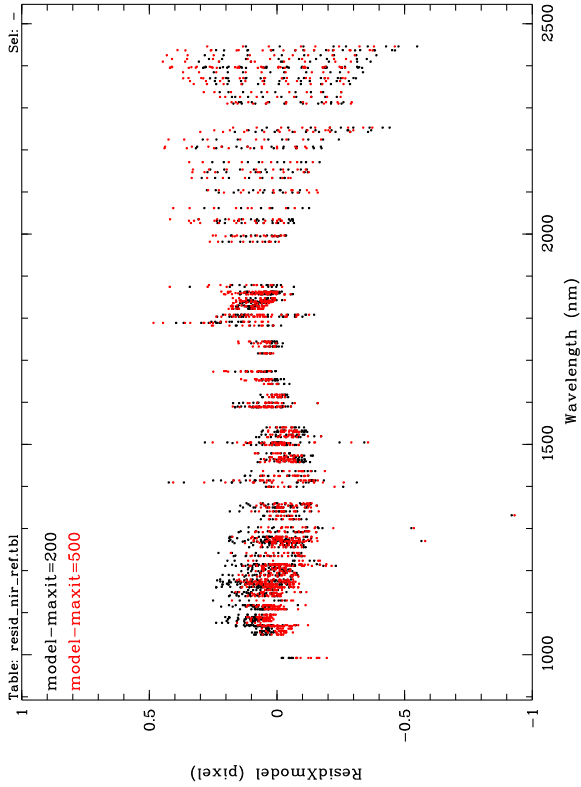


Figure 10: The plots show the residuals in pixels along the X (left column, mostly spatial axis) and Y (right column, mostly dispersion axis) axis vs. wavelength for the results of xsh_2dmap for VIS (bottom row) and NIR (top row) demo data. The black dots are the results for 2000 iterations (model-maxit=200, reflex default), while the red dots are the results for 5000 iterations (model-maxit=500, pipeline default).

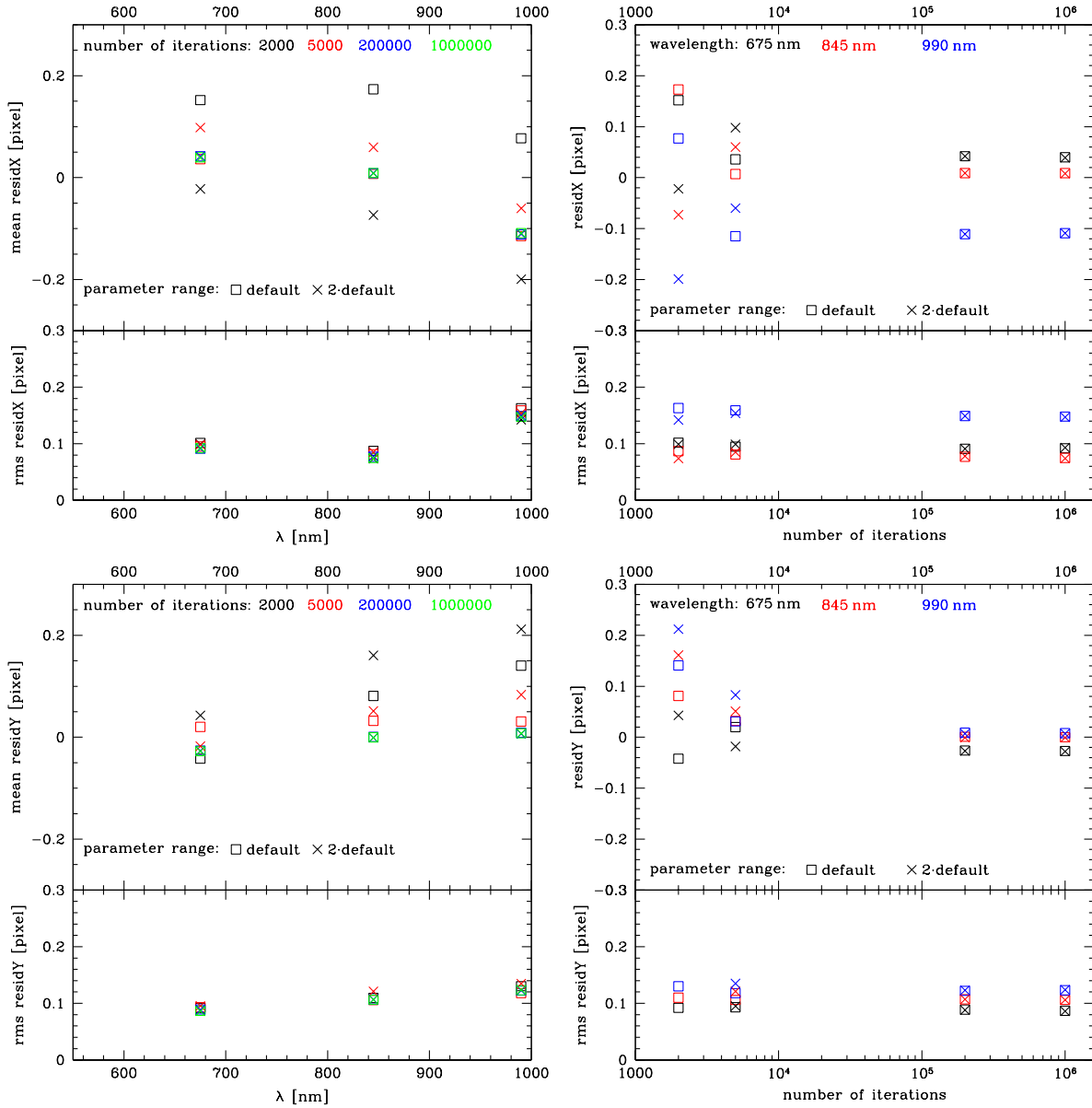


Figure 11: The plots show the average residuals in pixels and their rms along the X (mostly spatial axis, top row) and Y (mostly dispersion axis, bottom row) axis for the results of `xsh_2dmap` for VIS demo data vs. wavelength (left column) and number of iterations (right column). The residuals were averaged across the same wavelength ranges as the skyline residuals shown in Fig. 9 (p. 8). The open squares use the default parameter range for the model fit, while the crosses have that range increased by a factor 2.

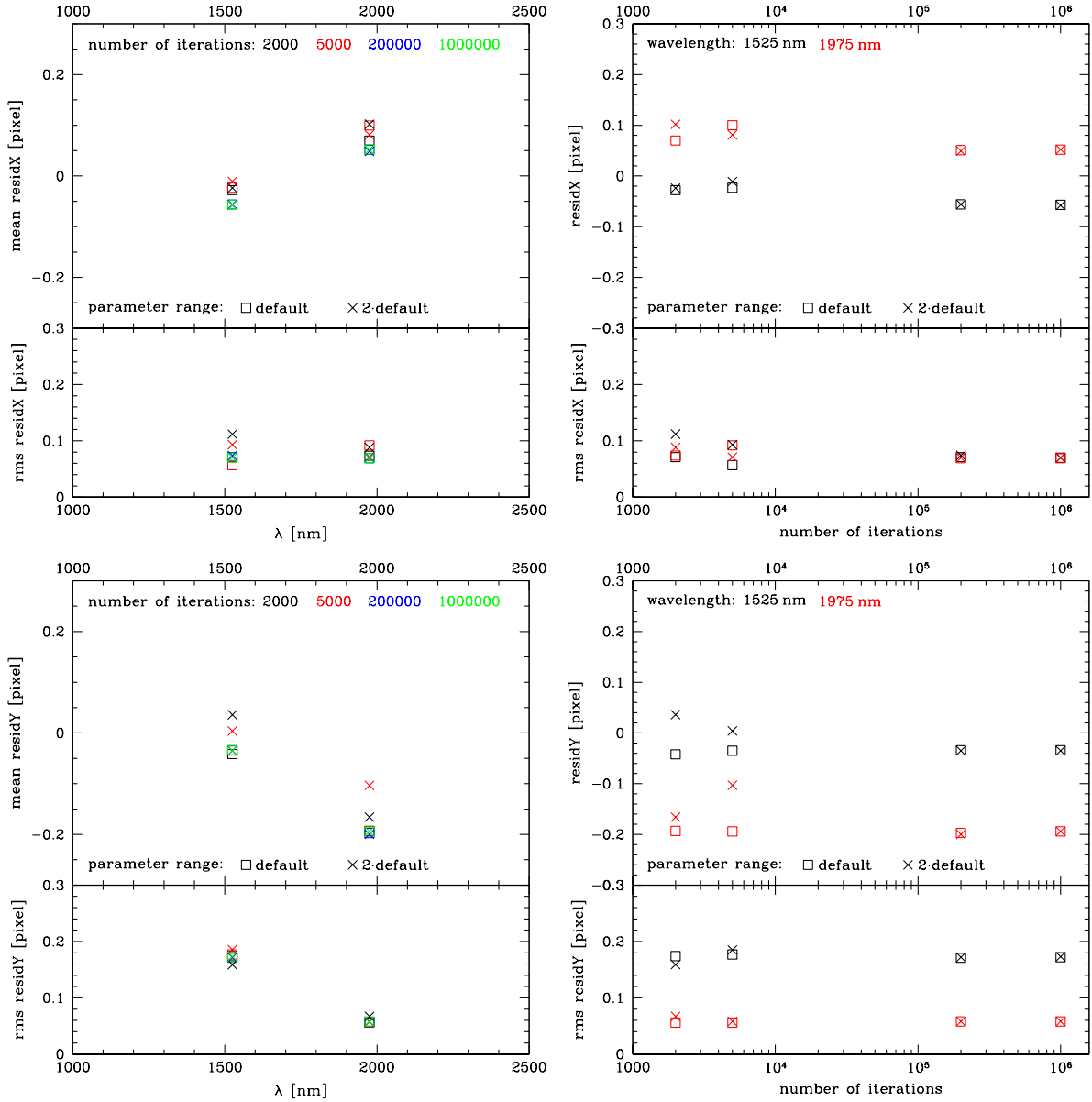


Figure 12: The plots show the average residuals in pixels and their rms along the X (mostly spatial axis, top row) and Y (mostly dispersion axis, bottom row) axis for the results of `xsh_2dmap` for NIR demo data vs. wavelength (left column) and number of iterations (right column). The residuals were averaged across the same wavelength ranges as the skyline residuals shown in Fig. 8 (p. 7). The bluest range from Fig. 8 gave no result with the `xsh_2dmap` results. The open squares use the default parameter range for the model fit, while the crosses have that range increased by a factor 2.

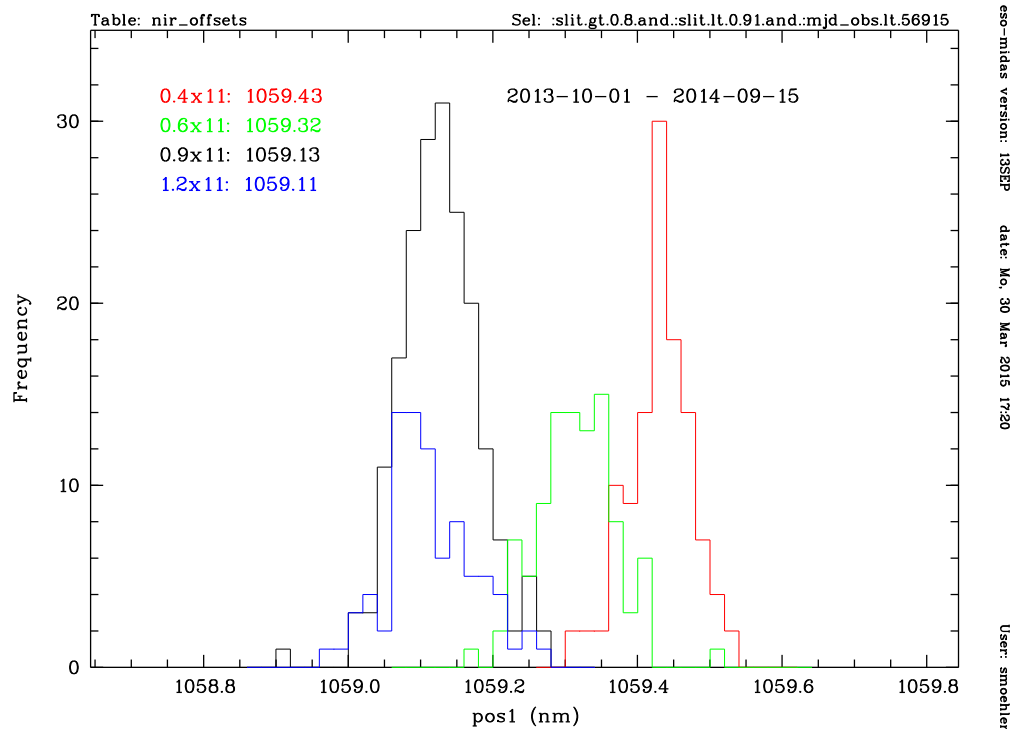


Figure 13: The plot shows the position of the arc line at $x \approx 1059$ pixel and $y = 603$ pixel in raw NIR arc slit frames. The histogram is similar to the one seen in Fig. 8 (p. 7).

decided to document the effect. Obviously these trends as well as the ones observed in the sky lines result in a systematic error, which is different from the systematic error caused by a rigid shift of the spectrum. As an estimate for the typical uncertainty caused by the trends in wavelength offsets I use the average across slits of the peak-to-peak variation in wavelength derived from sky lines. That results in a value of 0.28 pixel for both VIS and NIR data, which corresponds to 0.0056 nm and 0.0168 nm, respectively.

Currently, the systematic errors in wavelength are set to 0.03 nm (UVB), 0.02 nm (VIS), and 0.004 nm (NIR). This can be compared to the average of the wavelength shifts across slits and wavelength regions, which is -0.085 pixel for VIS data (-0.017 nm, dominated by the shifts observed at the red end) and -0.058 pixel for NIR data (-0.0035 nm, dominated by the shift in the central region). So the order of magnitude for the average shift is correct.

3.1 Slit Dependent Wavelength Shifts for NIR data

For the wavelength shifts derived from sky lines for NIR two distinct groups can be seen in Fig. 8 (p. 7), with the shifts from the slits 0.4x11, 0.6x11, and 0.9x11JH on one side and the shifts from the slits 0.9x11 and 1.2x11 on the other side, with a difference of about 0.25–0.3 pixels between them. A similar distribution can be seen in arc lamp frames observed with these slits. I measured the position of three arc lines (at $x \approx 1059, 1119, 1145$ pixel) in row 603 in the raw arc lamp frames with a Gaussian fit. The results for the line at $x \approx 1059$ pixels can be seen in Fig. 13 (p. 12). This suggests a possible mispositioning of the NIR slits.

C. Martayan noticed that the two groups of slits differ by the direction in which the slit wheel is moved to put them into the beam.

In order to find out since when the split in offsets has been present I performed the same measurements on arc slit frames since start of operations. The results are plotted in Fig. 14 and show that the split was introduced in July 2011, when a new slit wheel was installed, which provided two new slits with 0.6" and 0.9" width and a K-band blocking filter.

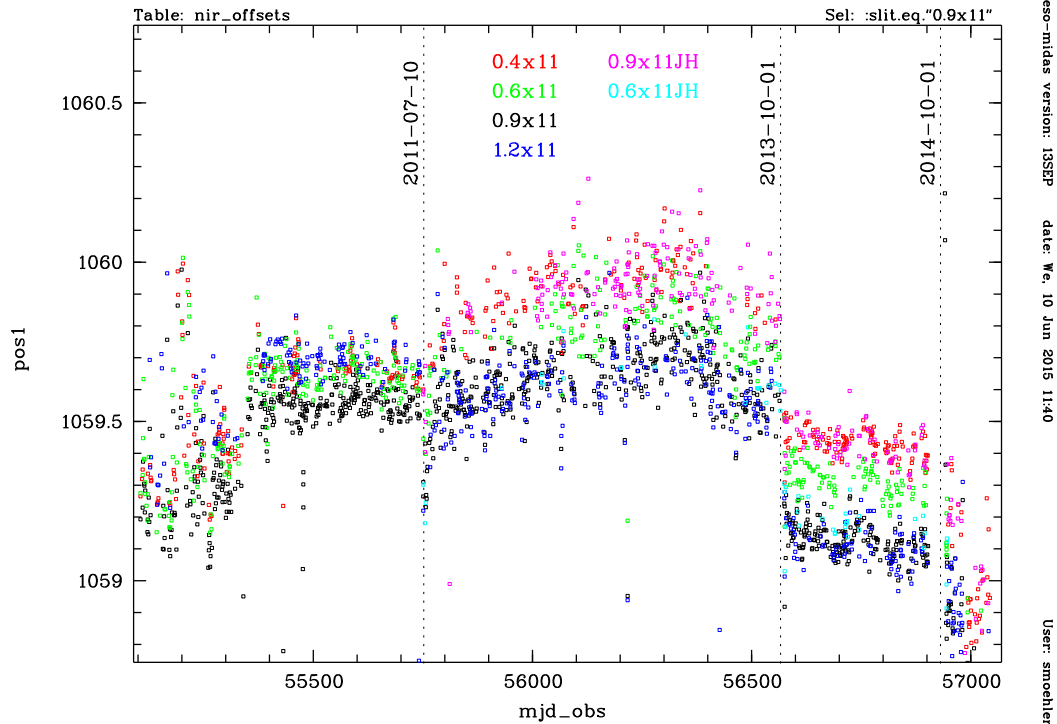


Figure 14: The plot shows the position of the arc line at $x \approx 1059$ pixel and $y = 603$ pixel in raw NIR arc slit frames vs. time. In July 2011 a new slit wheel was inserted. On October 1, 2013 X-shooter started operations at UT3. On October 1, 2014 X-shooter was back at UT2.

3.2 Overlap region between VIS and NIR

In order to look for possible inconsistencies between VIS and NIR skyline positions in their overlap regions I plot the offsets determined at 1020 nm (NIR) vs. those determined at 975 nm (VIS) in nm (see Fig. 15, p. 14). One can see that the offsets derived from the NIR data split into two groups depending on the slit used, while there is no such distinction for the VIS data. The fact that the VIS scatter around -0.05 nm (-0.2 pixel) can be understood from differential offsets shown in Fig. 9 (p. 8), which show an offset of -0.2 pixel for the red end of VIS data.

4 Offsets observed for telluric lines. II

To verify the effect of the changes in version 2.5.5 on the telluric line offsets I processed the 450 datasets each for VIS and NIR mentioned above, this time with sky subtraction. Some of the datasets, however, were too noisy to measure the positions of the telluric lines. The telluric line positions were measured by cross-correlating a part of the spectrum with a telluric model spectrum. For the VIS and NIR arm I used the ranges 927.06 nm–980.78 nm and 1097.62 nm–1211.94 nm, respectively. The NIR arm data show an offset of about -0.5 pixels (with some variation with the slit used), while the picture is less clear for the VIS arm data. Here the narrow slits (0.4x11 and 0.7x11) show an offset of 0.3–0.4 pixels, while the wider slits show no significant offset. The wider distribution in the VIS arm compared to the NIR is at least in part due to the smaller pixel size (0.02 nm for VIS vs. 0.06 nm for NIR data).

A discussion with C. Martayan (Instrument Scientist, IS) and A. Mehner (IF) yielded the following information:

- Before December 2013 the positioning problem went unnoticed.
- December 15, 2013 PPRS-054092 was opened to define a new set of reference pixels after C. Martayan (IS) found a drift of the reference pixels, which resulted in bad centering within the slit.
- January 11, 2014 PPRS-054092 was updated to report a further drift in negative y direction, i.e. mostly along the dispersion axis.

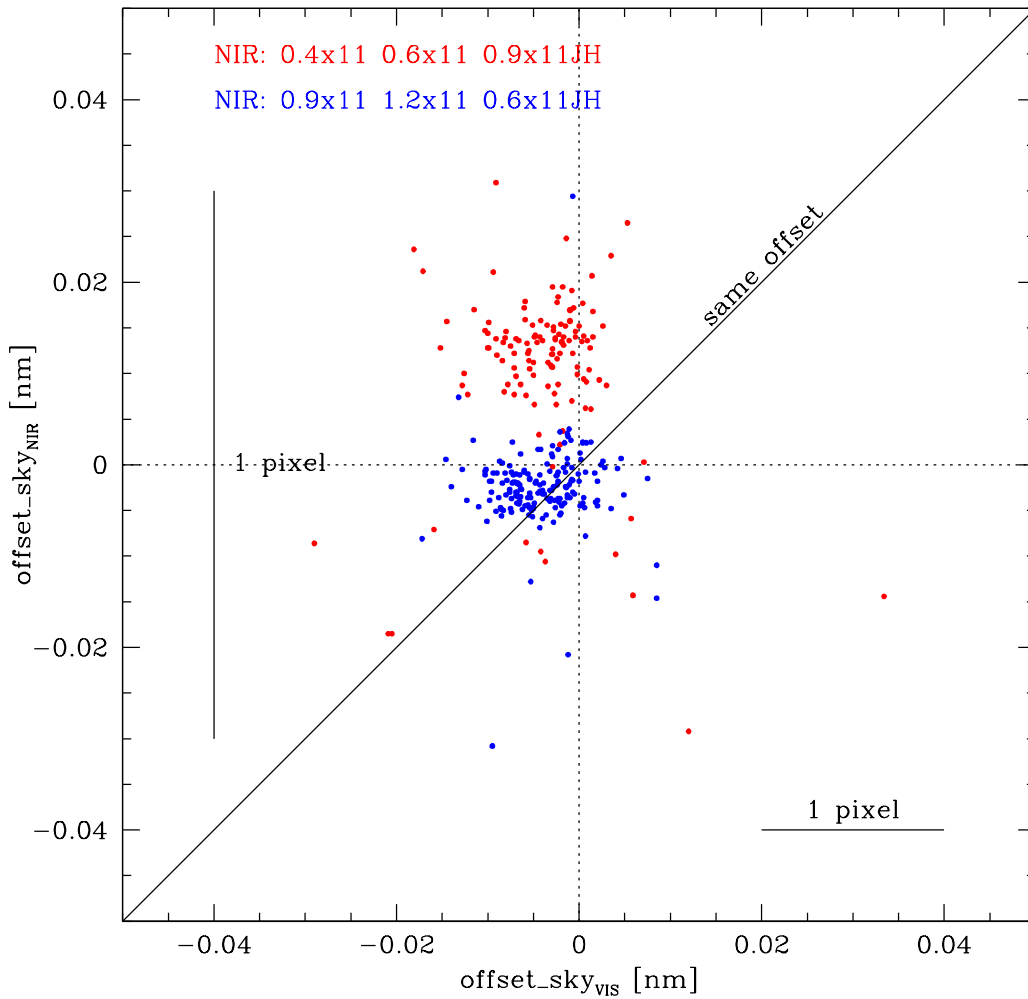


Figure 15: The plot shows the offsets (in nm) determined from sky lines at the red end of the VIS range (990 nm) and at the blue end of the NIR range (1020 nm) for the first data observed within a given template.

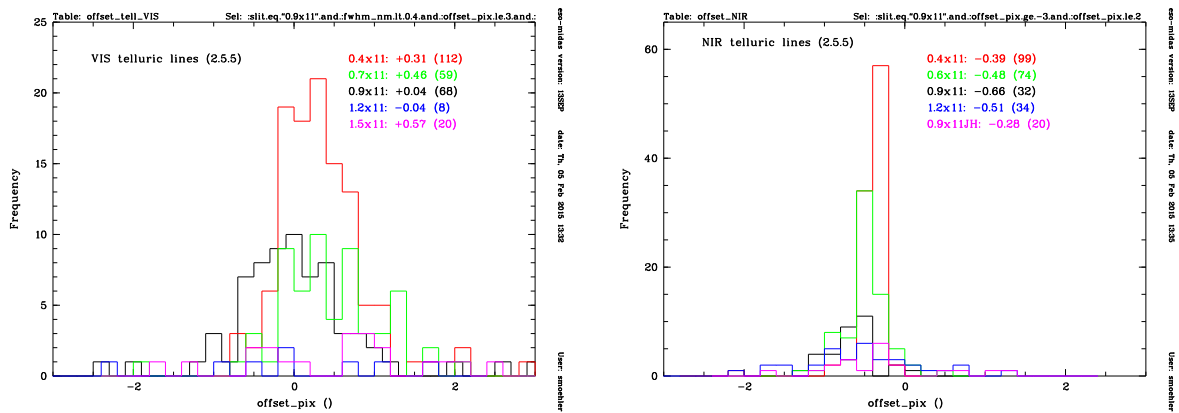


Figure 16: The plots show the histograms (VIS (left), NIR (right)) of telluric line offsets (in pixels) as determined from science data taken at UT3 and processed with pipeline version 2.5.5 which were cross-correlated with a telluric model spectrum.

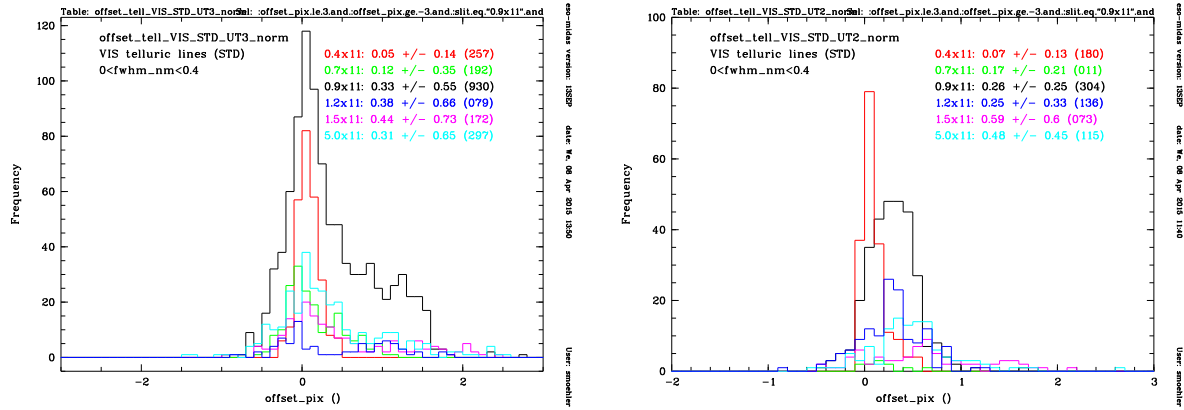


Figure 17: The plot shows the histograms of offsets as determined from QC processed (version 2.5.4) VIS observations of telluric and flux standard stars, which were cross-correlated with a telluric model spectrum. The left plot shows the results for observations between 2013-10-01 and 2014-09-30 (UT3) and the right one shows the results for observations between 2014-10-01 and 2015-02-25 (UT2).

- September 30, 2014 As part of the close-out at UT3 the reference pixels were verified by A. Mehner (IF), who found that the drift continued in the same direction. In addition she found that the reference pixels for the acquisition filters g' and U had not been corrected as requested by PPRS-054092. The target centering was off by -1.4 pixels ($0.24''$) for the g' filter and -2 pixels ($0.35''$) for the U filter until X-shooter moved to UT2, which caused flux losses up to 50% in the most narrow slits.
- October 2014 All reference pixels have been corrected.

One should keep in mind that also UVB data will be affected by incorrect reference pixels, even though the lack of telluric lines make the effect hard to detect.

This might explain why the offsets were seen in the earlier data shown in Figs. 1 (p. 2) and 2 (p. 2). Therefore I checked the offsets from QC processed spectra of telluric and flux standard stars observed at UT2 since 2014-10-01 (see Fig. 17, p. 15). I selected telluric standard stars because the results from the science were inconclusive due to many noisy spectra.

I had to use a different wavelength range for cross-correlation (715 nm-734 nm vs. 927 nm-980 nm for science data), probably due to the presence of Paschen lines in the telluric standard star spectra. Looking at Fig. 9 (p. 8) one finds a relative offset between the blue and red end of VIS spectra so that they are bluer by about 0.2 pixel at 990 nm compared to 700 nm. This should be kept in mind when comparing the results from the science data to those from the standard stars. I also noticed that the slope of the (hot) standard stars can cause problems, so I normalized the spectra with a linear fit across the telluric region used for the cross-correlation. To enable a better comparison between results from UT3 and UT2 I performed the same procedure for QC processed standard star spectra observed between 2013-10-01 and 2014-09-30.

The changes between the VIS data taken before/after October 2014 are less clear than I hoped.

For NIR data I could not use the QC processed data, as those were affected by the non-application of the AFC derived shifts. Therefore I processed the standards stars (telluric and flux) observed in the NIR arm between 2014-10-01 and 2015-02-25. I then normalized both these data and the science spectra from UT3 with a linear fit across the telluric region used for the cross correlation. The results can be seen in Fig. 18 (p. 16)

Also for the NIR arm the changes are not clear, but one should keep in mind that twice as many observations were analysed from UT2 compared to UT3 and the telluric standard stars generally have a better signal-to-noise ratio than the average science frame. For the NIR arm data from UT2 one may see a split between the offsets, depending on the slits used.

This check should be repeated by October 2015, when X-shooter has been at UT2 for year.

5 Conclusions

The results of my analysis can be summarized as follows:

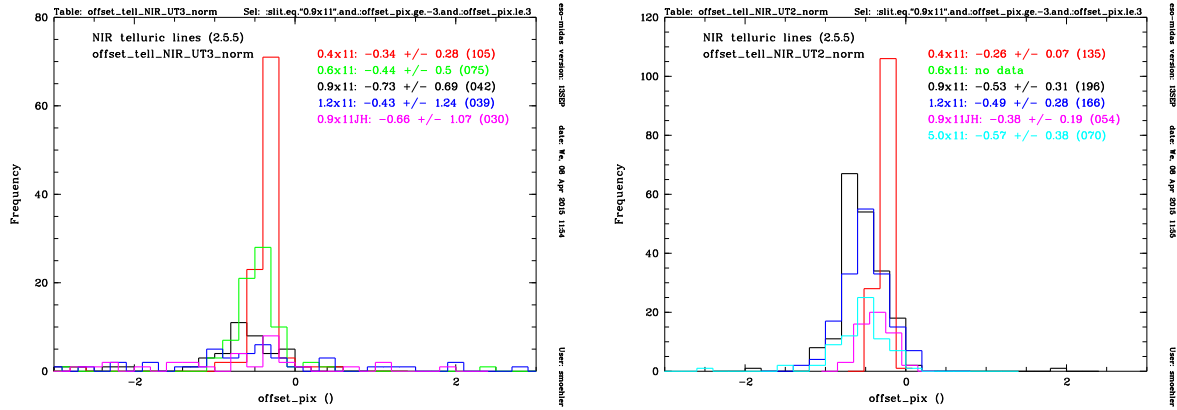


Figure 18: The plot shows the histograms of offsets as determined from NIR observations, which were cross-correlated with a telluric model spectrum. The left plot shows the results for science observations between 2013-10-01 and 2014-09-30 (UT3) and the right one show the results for standard star observations between 2014-10-01 and 2015-02-25 (UT2).

- The offsets observed for telluric lines depend on the slit width used and were at least partly caused by positioning problems, which have been fixed in October 2014. Data taken since then, however, still show shifts. UVB are also affected by problems with the reference pixels, even though the effect is much harder to notice due to the lack of telluric lines.
- Part of the shifts seen in NIR sky lines was due to the lack of AFC correction, which has been fixed in pipeline version 2.5.5.
- Both VIS and NIR data show wavelength dependent shifts with an average *peak-to-peak amplitude* of about 0.28 pixels, corresponding to 0.0056 nm and 0.0168 nm for VIS and NIR data, respectively.
- The *average* shifts observed for VIS and NIR data are consistent with the systematic error recorded in the pipeline products.
- The sky line offsets in the NIR data split into two groups, depending on the slit used for the observations. The groups consist of the slits 0.4x11, 0.6x11, 0.9x11JH on one side and 0.9x11, 1.2x11, 0.6x11JH on the other side. The effect is less clearly visible in telluric lines, but is clearly seen in the arc lines in arc lamp slit spectra. The split was introduced with the new slit wheel in July 2011.

Acknowledgments

Thanks go to (in alphabetical order) P. Bristow, C. Martayan, A. Mehner, and A. Modigliani for their help with this investigation.